

Efficient Path Interpolation and Speed Profile Computation for Nonholonomic Mobile Robots

Stéphane Lens¹ and Bernard Boigelot¹

Abstract—This paper studies path synthesis for nonholonomic mobile robots moving in two-dimensional space. We first address the problem of interpolating paths expressed as sequences of straight line segments, such as those produced by some planning algorithms, into smooth curves that can be followed without stopping. Our solution has the advantage of being simpler than other existing approaches, and has a low computational cost that allows a real-time implementation. It produces discretized paths on which curvature and variation of curvature are bounded at all points, and preserves obstacle clearance. Then, we consider the problem of computing a time-optimal speed profile for such paths. We introduce an algorithm that solves this problem in linear time, and that is able to take into account a broader class of physical constraints than other solutions. Our contributions have been implemented and evaluated in the framework of the Eurobot contest.

I. INTRODUCTION

The general problem of moving a mobile robot as fast as possible from a configuration to another while avoiding a given set of obstacles can be tackled by several methods, such as cell decomposition [3], roadmap [6], and potential field techniques [5]. In two-dimensional planar space, a large number of planning algorithms produce paths that are expressed as broken lines, i.e., sequences of straight line segments, between the initial and final configurations.

A differential-drive robot cannot follow such a path without stopping at the junction points between adjacent line segments in order to change its orientation, which wastes time. This problem can be alleviated by interpolating broken lines into smooth curves along which the orientation of the robot and the curvature remain continuous everywhere. This paper first addresses the problem of computing such interpolations, so as to obtain paths that can be physically followed without the need for stopping or slowing down excessively. We consider the case of differential-drive robots, but our results also apply to tricycle or car-like platforms. We develop an interpolation algorithm that guarantees that the obstacles cleared by a broken line are avoided as well by the resulting smoothed out path.

Once an interpolated path has been obtained, we then address another problem which consists in computing a time-optimal speed profile for it, i.e., associating each point of the curve with a timestamp that provides the instant at which it will be visited, in such a way that the total time needed for following the path becomes as small as possible. This computation has to take into account various physical constraints of the robot, e.g., bounds on its velocity or

acceleration measured at its wheels or its center of mass, limits imposed by the steering mechanism, . . . Some of these constraints may be context-sensitive, e.g., a tight speed bound may be imposed in the vicinity of obstacles cleared by a small margin, or steering constraints may be expressed as a function of the robot velocity.

Our motivation for studying these problems originates from our participation to the Eurobot² contest, in which autonomous mobile robots compete in a short-duration game played on a $2 \times 3 \text{ m}^2$ area. For this application, it is essential to plan paths in real-time due to the dynamic nature of obstacles, which practically requires a method with a computational cost limited to milliseconds of CPU time, as well as to obtain trajectories that minimize the time needed for moving the robot from one configuration to another. This prompted the development of a time-optimal speed profile computation algorithm that takes into account all the relevant physical constraints, such as those limiting traction at the robot wheels, or needed for ensuring stability in turns. Another requirement that is specific to the Eurobot application is to receive detailed and precise information about the locations that will be visited by the robot and their associated timestamps before starting to follow a trajectory, in order to be able to coordinate complex actions such as actuations carried out when the robot is moving, or jointly performed by two partner robots. While other approaches such as [7] and [8] have been proposed to deal with some of these requirements, our solutions are, to the best of our knowledge, the first ones that meet all of them in a satisfactory way. Our algorithms have been implemented and evaluated in the robots that we have built for Eurobot since 2008, which amounts to hundreds of thousands of trajectories successfully synthesized.

II. PROBLEMS STATEMENT

A. Interpolation Problem

The first problem that we consider consists of smoothing out a path expressed as a broken line. We define a *broken line path* as a sequence p_0, p_1, \dots, p_n of points, with $n \geq 1$, such that

- each point p_i , with $i \in [0, n]$ is defined by its coordinates (x_i, y_i) in two-dimensional space, and
- each intermediate point p_i , with $i \in [1, n - 1]$, is associated with a *clearance parameter* $c_i \in \mathbb{R}_{>0} \cup \{+\infty\}$.

The path is composed of the successive straight line segments $[p_0, p_1]$, $[p_1, p_2]$, . . . , $[p_{n-1}, p_n]$. In order to deal

¹Montefiore Institute, B28, University of Liège, B-4000 Liège, Belgium, {lens,boigelot}@montefiore.ulg.ac.be.

²<http://www.eurobot.org>

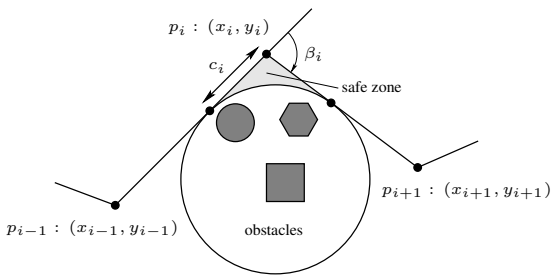


Fig. 1. Safe zone between adjacent segments

with obstacles, we assume that robots have zero measure, in other words, that a path clears a set of obstacles iff the intersection between its line segments and the union of all these obstacles is empty. (The case of robots with a cylindrical geometry can straightforwardly be handled by dilating obstacles.) The purpose of the clearance parameter c_i is to provide additional information about the location of the obstacles that are avoided when moving along the segments $[p_{i-1}, p_i]$ and $[p_i, p_{i+1}]$. This is achieved by considering a disk D_i that is tangent to both segments (which implies that its center belongs to the inner bisector of the angle formed by these segments), and that fully covers the obstacles cleared by the pair of segments. This latter property precisely means that the area located between the disk D_i and the segments $[p_{i-1}, p_i]$ and $[p_i, p_{i+1}]$ is free from obstacles; we call this area the *safe zone* of this pair of segments. (By extension, we consider that the segments themselves also belong to their safe zone.) The point is that any interpolation of the path that is confined to safe zones is guaranteed to avoid obstacles. The safe zone across p_i is characterized by the parameter c_i , defined as the distance between p_i and the points of tangency between D_i and the segments $[p_{i-1}, p_i]$ and $[p_i, p_{i+1}]$. This parameter may be left undefined ($c_i = +\infty$), in which case its value can be replaced by the smallest of the lengths of the two segments. (In other words, D_i is then the largest disk simultaneously tangent to both segments.) An illustration is provided in Figure 1.

For each $i \in [1, n-1]$, we define β_i as the angle between the vectors $\overrightarrow{p_{i-1}p_i}$ and $\overrightarrow{p_i p_{i+1}}$, which corresponds to the change in orientation of the robot when it moves from the segment $[p_{i-1}, p_i]$ to the segment $[p_i, p_{i+1}]$. Without loss of generality, we assume $\beta_i \neq 0$. It is also natural to impose an upper bound on $|\beta_i|$. Indeed, with a large value of β_i , the segments $[p_{i-1}, p_i]$ and $[p_i, p_{i+1}]$ can be followed in opposite directions, and it is not always appropriate in such cases to interpolate the path into one that remains close to the segments. In this work, we arbitrarily impose the upper bound $|\beta_i| \leq \pi/2$ for all $i \in [1, n-1]$. In the case of adjacent segments forming an acute angle, it then becomes necessary to interleave an intermediate segment between them.

A differential-drive robot subject to physical constraints cannot follow a broken line path without stopping at junction points. Such constraints usually take the form of lower and upper bounds on the velocity and acceleration of the robot measured at specific locations, such as its individual wheels,

center of mass, or other reference centers. The speed that can be reached by the robot at some point of a path is then bounded by a function of the absolute curvature $|\kappa|$ at this point, as well as the rate of variation $|d\kappa/ds|$ of this curvature with respect to the linear traveled distance.

We are now ready to define precisely the interpolation problem. Given a broken line path, the goal is to compute a curve that leads from its origin to its endpoint staying within safe zones, and such that the absolute curvature and variation of curvature remain small at all points. For our intended applications, it is essential to be able to carry out this operation with a low computational cost. Finally, one must be able to discretize the resulting interpolated path. This discretization must be physically sound, in the sense that the discretized values of the physical variables of interest (such as speeds and accelerations) must remain close to their actual value.

B. Speed Profile Problem

The second problem that we address takes as input a discretized path, expressed as a sequence of configurations (x_i, y_i, θ_i) successively visited by a robot, where (x_i, y_i) denotes the two-dimensional coordinates of its reference center, and θ_i its absolute orientation. In addition, some number of physical constraints that need to be satisfied at all times are provided, such as lower and upper bounds on the velocity or acceleration of individual wheels, the speed, angular speed, and tangential and radial accelerations measured at the center of mass or some other reference points, on the rate of variation of the steering angle for a tricycle robot, ... Some of those constraints may be context-sensitive, such as imposing tighter speed bounds in the vicinity of some obstacles, or expressing the admissible angular velocity of the steering wheel as a function of the robot speed. Besides those constraints, the initial speed of the robot is specified at the origin of the path, together with an upper bound on the speed that can be reached at its endpoint. Given a path and a set of physical constraints, the aim is to compute for all visited configurations (x_i, y_i, θ_i) a timestamp t_i that defines the time at which this configuration will be reached, starting from $t_0 = 0$. The goal is to obtain the speed profile that minimizes the total time needed for following the path, while satisfying the physical constraints at all times.

III. PATH INTERPOLATION

We solve the interpolation problem in two steps, the first one being aimed at producing a path in which the absolute curvature is bounded at all points, and the second one modifying this path in order to now bound the rate of variation of curvature. In both steps, the interpolated path has to stay within safe zones in order to clear obstacles.

A. Bounding Curvature

In order to bound absolute curvature, we build a curve composed of straight line segments (with zero curvature) and circle arcs (with constant curvature), connected in such a way that continuity of the tangent vector is ensured everywhere.

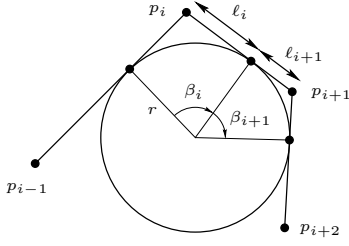


Fig. 2. Segments tangent to a common circle

On such a curve, the curvature can be expressed as a piecewise constant function with respect to traveled distance.

We construct such a curve by computing, for each pair of adjacent segments $([p_{i-1}, p_i], [p_i, p_{i+1}])$ a value ℓ_i specifying the distance from p_i at which the curve transitions from the segments to a circle arc. In other words, ℓ_i corresponds to the distance between p_i and each point of tangency between that circle arc and the segments.

Of course, in order to clear obstacles, it is necessary to have $\ell_i \leq c_i$ for all $i \in [1, n-1]$. We compute ℓ_i by applying the following principle: If three or more consecutive segments are all tangent to a common circle, then the arcs that interpolate these segments must belong to that circle, provided that they are located within safe zones. This solution has the desirable property of keeping the curvature constant across two or more interpolation steps.

We now show how to carry out this computation. Consider a path in which all segments are tangent to a common circle of radius r . This situation is illustrated in Figure 2. At the points p_i and p_{i+1} , one has respectively $\ell_i = r |\tan(\beta_i/2)|$ and $\ell_{i+1} = r |\tan(\beta_{i+1}/2)|$. Since, in this case, the constraint $\ell_i + \ell_{i+1} = |p_i p_{i+1}|$ is satisfied, we obtain

$$\ell_i = \frac{\tau_i |p_i p_{i+1}|}{\tau_i + \tau_{i+1}} \quad (1)$$

$$\ell_{i+1} = \frac{\tau_{i+1} |p_i p_{i+1}|}{\tau_i + \tau_{i+1}}, \quad (2)$$

where $\tau_i = |\tan(\beta_i/2)|$ for all i . Note that these expressions do not involve r , and that Equation (1) can be rewritten at the point p_i into

$$\ell_i = \frac{\tau_i |p_{i-1} p_i|}{\tau_{i-1} + \tau_i}. \quad (3)$$

For general paths, successive segments are not tangent to a common circle, and Equations (1) and (3) then provide different values for ℓ_i . Our strategy is, for all $i \in [1, n-1]$, to define ℓ_i as the smallest value among those expressed by Equations (1) and (3), and the clearance parameter c_i . This solution also applies to pairs of adjacent segments that turn in opposite directions; in such a case, small values of $|\beta_i|$ (which represent small changes of direction) lead to small circle arcs, and large values of $|\beta_i|$ to large arcs, which is geometrically sound.

B. Bounding Curvature Variations

We now turn to the problem of modifying the path produced at the previous step, which has a curvature that

is piecewise constant, into one in which the rate of variation of curvature with respect to traveled distance remains bounded. Clearing obstacles is achieved by constraining the interpolation to remain within safe zones. The resulting path must have a curvature that is continuous, bounded, and of bounded slope, at all points.

We construct such curves out of *clothoids*, which correspond to the paths followed by differential-drive robots when their wheels are driven at respectively their minimum and maximum acceleration (as a result, for instance, of bang-bang control). Clothoids are formally defined as curves with a curvature that varies linearly with traveled distance. The coordinates of the points visited by a clothoid are expressed in terms of Fresnel integrals, which cannot be evaluated analytically, but for which very efficient numerical approximations are known [12].

Consider a circle arc with curvature κ_C , interpolating two successive line segments $[p_{i-1}, p_i]$ and $[p_i, p_{i+1}]$ within their safe zone. Assuming w.l.o.g. $\kappa_C > 0$ (the case $\kappa_C < 0$ is handled symmetrically), we have established the following result.

Theorem 1: For every curvatures κ_1, κ_2 such that $0 \leq \kappa_1 < \kappa_C$ and $0 \leq \kappa_2 < \kappa_C$, there exist two clothoids arcs moving respectively from the curvatures κ_1 to κ_M and from κ_M to κ_2 , with $\kappa_M > \kappa_C$, the concatenation of which interpolates the path from p_{i-1} to p_{i+1} within the safe zone, with continuity of the tangent vector at the junction point between the two curves. The parameters of these two clothoids arcs are uniquely determined by $\kappa_1, \kappa_2, \kappa_C$, and the rotation angle β_i .

Our method for characterizing the two clothoid arcs consists in reasoning on a diagram expressing the curvature of the interpolated path as a function of traveled distance. The problem is illustrated in Figure 3 (exaggerating the curvatures in order to make the interpolated path stand out from the circle arc). Let s_M denote the distance traveled along the first arc, and s_F the total distance traveled over both arcs. The linear rate of variation of curvature for these arcs are respectively denoted by d_1 and $-d_2$. In the graph depicted in Figure 3(b), the area below the curvature line must be equal to β_i . Note that s_M and κ_M can be expressed in terms of the other variables, since one has $\kappa_M = \kappa_1 + d_1 s_M = \kappa_2 + d_2 (s_F - s_M)$.

It thus remains to compute d_1, d_2 and s_F given κ_1, κ_2 and β_i . We solve this problem numerically, observing empirically that the initial estimate

$$\frac{s_F}{s_M} = 1 + \frac{\kappa_C - \kappa_1}{\kappa_C - \kappa_2}$$

leads to very fast convergence with Newton-Raphson's method. In practice, we first perform a variable change operation by defining

$$a = \frac{d_1 - d_2}{d_1 + d_2} \quad \text{and} \quad d = \frac{d_1 + d_2}{2},$$

and then carry out the search over the variables s_F, a , and d . Intuitively, a is a measure of the asymmetry between the two clothoids arcs, and remains small when κ_1 and κ_2

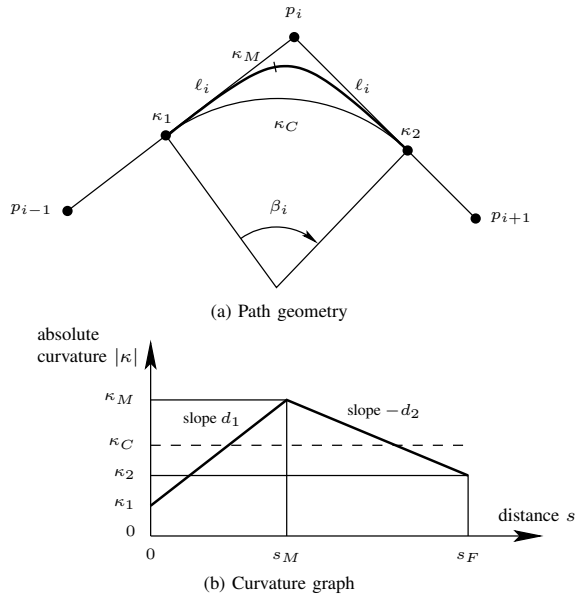


Fig. 3. Interpolation with two clothoid arcs

are reasonably balanced. The value of s_F is confined to an interval with a lower bound β_i/κ_C equal to the distance traveled on the circle arc. Its upper bound corresponds to the minimum value among

$$\frac{2}{\kappa_C} \tan \frac{\beta_i}{2} \quad \text{and} \quad \frac{\beta_i}{\min(\kappa_1, \kappa_2)},$$

which respectively correspond to the combined length of the line segments, and the largest distance that can be traveled without lowering the curvature below κ_1 and κ_2 . It is also worth mentioning that, in the particular case $\kappa_1 = \kappa_2 = 0$, this procedure can be simplified into one that does not rely on approximations [1], except for evaluating Fresnel integrals.

Finally, in order to apply Theorem 1, it remains to choose values for κ_1 and κ_2 at the extremities of interpolated curves. We use the following strategy:

- At the junction between a straight line segment and an arc, or between two arcs turning in opposite directions, a natural choice is $\kappa_i = 0$.
- If we need to connect two arcs turning in the same direction, with respective curvatures κ_{C1} and κ_{C2} which we assume w.l.o.g. to be positive, we have to choose a curvature κ_i that satisfies $\kappa_i < \min(\kappa_{C1}, \kappa_{C2})$. This can be achieved by defining $\kappa_i = f \min(\kappa_{C1}, \kappa_{C2})$, where $0 < f < 1$ is a reduction factor that can be arbitrarily chosen. For the Eurobot application, we have observed that selecting $f = 0.70$ leads to paths along which both the curvature and variation of curvature stay within acceptable bounds.

IV. SPEED PROFILE COMPUTATION

Before addressing the computation of a speed profile for a given path, we need to define the formalism in which such paths are represented. As explained in Section II-B, a discretized path takes the form of a sequence (x_0, y_0, θ_0) ,

$(x_1, y_1, \theta_1), \dots, (x_m, y_m, \theta_m)$ of successive configurations of the robot sampled at indices ranging from 0 to m . The discretization step between these configurations is usually much finer than for specifying the broken lines that are input to the interpolation procedure described in Section III. (In the Eurobot application, the clothoid arcs synthesized by this procedure are each typically discretized into dozens of intermediate configurations.) This strategy differs from methods such as [7] and [13], in which curves are represented in analytic form. The advantages of our approach are that discretized trajectories can be handled with much simpler data structures, are not limited to curves that admit an analytic form, and are less subject to numerical issues. We stress the fact that the speed profile computation algorithm discussed in this section is not restricted to the paths considered in Section III, but is applicable to arbitrary curves, in particular to those produced by techniques such as [13].

Let us now discuss the precise semantics of discretized paths. Between a configuration (x_i, y_i, θ_i) and its successor $(x_{i+1}, y_{i+1}, \theta_{i+1})$, we consider that the robot moves along a circle arc, increasing its orientation by the angle $\delta_i = \theta_{i+1} - \theta_i$, which is usually small in the case of fine discretization. This circle arc is fully characterized by the angle δ_i together with the chord length

$$\lambda_i = \sqrt{(x_{i+1} - x_i)^2 + (y_{i+1} - y_i)^2}.$$

The curvature κ_i at this step thus satisfies

$$\kappa_i = \frac{2}{\lambda_i} \sin \frac{\delta_i}{2}.$$

For the sake of simplicity, and in order to be able to easily chain paths together, we impose this curvature to be zero at the origin and endpoint of all paths.

Recall that the aim is to obtain a speed profile for a given path that minimizes the total time needed for following this path. We build such a profile by computing the largest possible value for the speed of the robot at each index from 0 to m . This speed can potentially be measured at various locations on the robot, such as its center of mass, its wheels, ... For differential-drive, tricycle or car-like robots, all those speeds can be expressed as functions of a single parameter and the geometry of the path. A natural choice would be to define this parameter as the speed of the robot measured at its center which, in the case of differential-drive robot, is defined as the midpoint of the line segment linking the two locomotion wheels. This solution turns out to be problematic for reasoning about parts of paths where the absolute curvature is high, which intuitively corresponds to rotations of the robot around its center. In such a case, even though the robot is in motion, its center moves only slowly, or not at all.

We choose instead to express all speeds of interest in terms of a parameter z_i that we call the *velocity* at the current index i of the path, defined as the quadratic mean of the respective speeds v_{Li} and v_{Ri} of the left and right wheels of

the differential drive:

$$z_i = \sqrt{\frac{v_{Li}^2 + v_{Ri}^2}{2}}.$$

This parameter has the advantage of being always positive, and nonzero whenever the robot is not stationary. Knowing the geometry of the robot, one can easily compute the speeds at its center, center of mass, individual wheels, or other locations of interest, from the velocity z_i and the curvature κ_i at the current path index. When the curvature is zero, such as at the extremities of paths, all those speeds become equal to z_i .

This reduces the speed profile computation problem to determining, for each index i , the highest possible velocity z_i at that point. Note that one cannot realistically assume that this velocity remains constant when the robot follows the circle arc from (x_i, y_i, θ_i) to $(x_{i+1}, y_{i+1}, \theta_{i+1})$. Indeed, the speed of the robot would then be discontinuous at the junction points between adjacent arcs, which would complicate the handling of acceleration constraints.

A better solution is to consider that, between the indices i and $i+1$, the velocity varies linearly from z_i to z_{i+1} with respect to traveled distance. With this assumption, all the accelerations of interest (such as those measured at individual wheels, at the center of mass or other locations, in the tangential or radial directions, ...) can be derived from the values of z_i , z_{i+1} , and κ_i , and take at all locations values that accurately approximate those of the underlying (undiscretized) curve, assuming a sufficiently fine discretization.

The physical constraints imposed on the robot can be classified in two groups. We first have constraints that translate into an upper bound on the velocity z_i at a path index i . Let us illustrate this situation with a simple example. Assume that the speeds v_{Ri} and v_{Li} measured at respectively the right and the left wheels of the differential drive (in the forward direction) are constrained to belong to the interval $[-v_{imax}, v_{imax}]$ at the path index i , with $v_{imax} > 0$. Expressing the wheel speeds in terms of z_i , we obtain $v_{Ri} = z_i\sqrt{2} \sin \omega_i$ and $v_{Li} = z_i\sqrt{2} \cos \omega_i$, where ω_i is defined as the angle that satisfies

$$\tan \omega_i = \frac{1 + \frac{e\kappa_i}{2}}{1 - \frac{e\kappa_i}{2}}, \quad -\frac{\pi}{4} < \omega_i < \frac{3\pi}{4},$$

and e is the distance between the wheels. The relations between v_{Ri} , v_{Li} , z_i and ω_i are illustrated in Figure 4. Our constraint then gives out the upper bound

$$z_i \leq \frac{v_{imax}}{\sqrt{2} \sin \omega_i} \quad \text{if } \frac{\pi}{4} < \omega_i < \frac{3\pi}{4},$$

$$z_i \leq \frac{v_{imax}}{\sqrt{2} \cos \omega_i} \quad \text{if } -\frac{\pi}{4} < \omega_i < \frac{\pi}{4}.$$

The second group of constraints contains those that involve the velocities z_i and z_{i+1} at two successive indices i and $i+1$. This group notably includes constraints expressed in terms of accelerations. Let us give an example. The tangential acceleration experienced at the center of a differential-drive

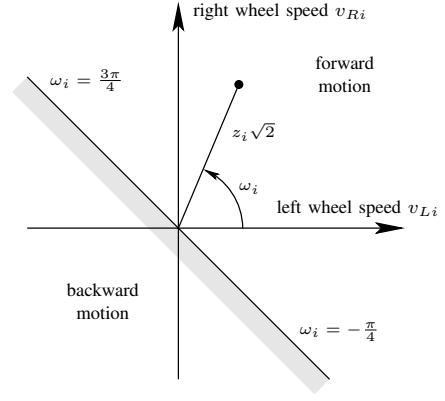


Fig. 4. Relations between speeds

robot during step i is given by

$$a_{Ti} = \frac{v_{i+1}^2 - v_i^2}{2s_i},$$

where v_i denotes the speed measured at the center at the path index i , and $s_i = \delta_i/\kappa_i$ is the distance driven during step i . Since we have $v_i = (v_{Ri} + v_{Li})/2$ for all i , this expression becomes

$$a_{Ti} = \frac{(\sin \omega_{i+1} + \cos \omega_{i+1})^2 z_{i+1}^2 - (\sin \omega_i + \cos \omega_i)^2 z_i^2}{4s_i},$$

where ω_i is defined as in the previous example. One easily sees that imposing bounds on this acceleration amounts to enforcing a constraint over both z_i and z_{i+1} . At all every path index $i \in [0, m-1]$, we denote by $\phi_i(z_i, z_{i+1})$ the conjunction of all physical constraints that jointly involve z_i and z_{i+1} . Note that constraints in both groups may be context-sensitive: The constraints involving z_i and z_j at two different locations i and j can differ, or be expressed with respect to different values of parameters. This makes it possible, for instance, to impose tighter speed limits in the close vicinity of obstacles.

We are now ready to describe our procedure for computing the fastest physically-feasible speed profile for a given path. This procedure has originally been introduced in [11]. It differs from [2], [7] by the much broader range of physical constraints that it supports. The algorithm proceeds in three stages. In the first one, it computes for every index i , the largest possible value z_{imax} allowed by the constraints of the first group at that point. It is also essential to make sure that the constraints that belong to the second group remain satisfiable: if z_{imax} is such that the constraint $\phi_i(z_{imax}, z_{i+1})$ does not hold for at least one $z_{i+1} \leq z_{i+1max}$, then z_{imax} has to be lowered into the largest value that makes the constraint satisfiable. In the same way, z_{imax} must be sufficiently small for the constraint $\phi_{i-1}(z_{i-1}, z_{imax})$ to be satisfiable in z_{i-1} . These operations can be carried out numerically, a simple strategy being to perform a binary search until the required precision is reached.

After a suitable value of z_{imax} has been obtained at all indices i , the second stage assigns a tentative value to z_i for

increasing values of i . The initial velocity z_0 is fixed by the speed of the robot specified at the origin of the path. Then for $i = 1, 2, \dots$, we successively compute the largest value of z_i that is less than or equal to the upper bound z_{imax} at the index i , and that satisfies the constraint $\phi_{i-1}(z_{i-1}, z_i)$ (with the value of z_{i-1} obtained at the previous step).

The third and last stage performs a similar operation for decreasing values of i , starting from the last index m of the path and moving towards its origin. Before the first iteration, the velocity z_m at the end of the path has possibly to be lowered in order to satisfy the upper bound imposed on the final speed of the robot. Then, for $i = m - 1, m - 2, \dots$, one successively adjusts the current value of z_i (by lowering it or leaving it unchanged) so as to satisfy the constraint $\phi_i(z_i, z_{i+1})$.

After completing this stage, the computed values of z_i at all path indices are such that constraints of both groups are satisfied, and it remains to check that the computed initial velocity z_0 corresponds to the initial speed of the robot. In the case of a mismatch (meaning that z_0 had to be lowered during third stage), it is impossible to follow the path with the specified initial speed while satisfying all physical constraints, and the speed profile computation returns an error. Otherwise, one can straightforwardly compute, from the value of z_i at all indices and the geometry of the path, the instant t_i at which the corresponding configurations will be reached.

This technique yields a time-optimal speed profile, since increasing the speed of the robot at any location on the path would lead to violating at least one physical constraint. The computational cost is linear in the number of path steps, provided that all constraints can be solved in bounded time.

V. CONCLUSIONS

In this paper, we have addressed the problem of interpolating a path expressed as a sequence of straight line segments into a trajectory that can be followed as fast as possible by a nonholonomic robot, taking into account the physical constraints of the robot. This problem has been well studied in the literature [9], [4], [10], [13], [8], [7], but our motivation for developing an original solution was prompted by the particular requirements of the Eurobot contest. In this setting, it is crucial to be able to plan trajectories that can be generated with very low computational cost, to take into account complex physical constraints such as those governing traction at individual wheels or ensuring stability in turns, and to provide accurate spatial and temporal advance information about the visited configurations. To the best of our knowledge, our solution is the first one that meets all those requirements. Compared with methods such as [14], [13] that also rely on clothoids for interpolating paths, our approach of joining only two arcs of clothoids for moving from one curvature to another has the advantage of being simpler and computationally cheaper, the trade-off being that the generated curves are not guaranteed to be optimal.

The path interpolation and speed profile computation algorithms discussed in this paper have been implemented in the

Discretized points	Synthesis time	Discretization time	Speed profile time	Total time
292	15.2 μ s	33.4 μ s	140.9 μ s	189.5 μ s
520	29.6 μ s	53.6 μ s	239.0 μ s	322.2 μ s
632	30.8 μ s	72.7 μ s	303.5 μ s	407.0 μ s
656	23.1 μ s	77.9 μ s	319.1 μ s	420.1 μ s

Fig. 5. Experimental results

robots built for Eurobot at the University of Liège since 2008, together with an original path planning algorithm. In this setting, they have been successfully validated on hundreds of thousands of trajectories, considering 16 distinct physical constraints of robots with differential as well as tricycle drive, some of them being context-sensitive: lower and upper bounds on the speed and acceleration of locomotion and steering wheels, on the speed, angular speed, tangential and radial accelerations at the center of mass, and on the angular rate of steering. In order to illustrate the efficiency of our method, we report in Figure 5 the time needed for running the interpolation and speed profile algorithms on a few sample trajectories experienced in the Eurobot application. We distinguish the costs of the curve synthesis, path discretization, and speed profile computation steps. The total computational cost typically amounts to less than half a millisecond of CPU time on a i5-460M processor running at 2.53 GHz, which is several orders of magnitude faster than techniques such as [7].

REFERENCES

- [1] M. Brezak and I. Petrović, "Path smoothing using clothoids for differential drive mobile robots," in *18th IFAC World Congress 2011*, Sept 2011, pp. 1133–1138.
- [2] —, "Time-optimal trajectory planning along predefined path for mobile robots with velocity and acceleration constraints," in *Advanced Intelligent Mechatronics (AIM), 2011 IEEE/ASME International Conference on*, July 2011, pp. 942–947.
- [3] R. Brooks and T. Lozano-Perez, "A subdivision algorithm in configuration space for findpath with rotation," *Systems, Man and Cybernetics, IEEE Transactions on*, no. 2, pp. 224–233, 1985.
- [4] H. Choset, K. M. Lynch, S. Hutchinson, G. Kantor, W. Burgard, L. E. Kavraki, and S. Thrun, *Principles of Robot Motion: Theory, Algorithms, and Implementations*. The MIT Press, 2005.
- [5] S. S. Ge and Y. J. Cui, "Dynamic motion planning for mobile robots using potential field method," *Autonomous Robots*, vol. 13, no. 3, pp. 207–222, 2002.
- [6] S. Karaman, M. R. Walter, A. Perez, E. Frazzoli, and S. Teller, "Any-time motion planning using the RRT*," in *Robotics and Automation (ICRA), IEEE International Conference on*, 2011, pp. 1478–1483.
- [7] T. Kunz and M. Stilman, "Time-optimal trajectory generation for path following with bounded acceleration and velocity," in *Robotics: Science and Systems VIII*, 2012.
- [8] Y. Kuwata, S. Karaman, J. Teo, E. Frazzoli, J. P. How, and G. Fiore, "Real-time motion planning with applications to autonomous urban driving," *IEEE Trans. on Control Systems Technology*, vol. 17, no. 5, pp. 1105–1118, 2009.
- [9] J.-C. Latombe, *Robot Motion Planning*. Kluwer, 1991.
- [10] S. M. LaValle, *Planning algorithms*. Cambridge Uni. Press, 2006.
- [11] S. Lens, "Locomotion d'un robot mobile," Master's thesis, Université de Liège, 2008.
- [12] K. D. Mielenz, "Computation of Fresnel integrals II," *J. Res. Natl. Inst. Stand. Technol. (NIST)*, vol. 105, no. 4, pp. 589–590, 2000.
- [13] A. Scheuer and T. Fraichard, "From Reeds and Shepp's to continuous-curvature paths," *IEEE Trans. on Robotics*, vol. 20, no. 6, pp. 1025–1035, 2004.
- [14] D. H. Shin and S. Singh, "Path generation for robot vehicles using composite clothoid segments," Robotics Institute, Carnegie Mellon University, Tech. Rep. CMU-RI-TR-90-31, December 1990.